

Reactions of $[M_2(CO)_{10}]$ ($M = Mn$ or Re) with xenon bis[pentafluorooxo-tellurate(vi) and -selenate(vi)]

Martin C. Crossman, Eric G. Hope* and Lee J. Wootton

Department of Chemistry, University of Leicester, Leicester, UK LE1 7RH

The oxidation of $[M_2(CO)_{10}]$ ($M = Mn$ or Re) with $Xe(OEF_5)_2$ ($E = Se$ or Te) in dichloromethane at room temperature afforded $[M(OEF_5)(CO)_5]$ ($M = Mn$ or Re , $E = Se$ or Te) which have been characterised by mass spectrometry, IR and NMR spectroscopies and extended X-ray absorption fine structure (EXAFS) spectroscopy

Pentafluorooxotellurate(vi) (teflate) is very versatile and has been used to co-ordinate to high-oxidation-state metals and non-metals and as a ligand for organometallic systems.^{1–3} The isoelectronic pentafluorooxoselenate(vi) (seflate) has only found relatively limited application; characterised complexes include $M[OSeF_5]$ ($M =$ alkali metal⁴ or NO_2 ⁵), $EOSeF_5$ ($E = F$ or Cl or Br),⁶ $Br(OSeF_5)_3$,⁶ $E(OSeF_5)_2$ ($E = Xe$ ^{7,8} or Hg ^{4,7}) and the transition-metal complexes $[TiF_{4-x}(OSeF_5)_x]$, $[VO(OSeF_5)_3]$ and $[CrO_2(OSeF_5)_2]$.⁹ This disparity in the range of chemistry established for these ligands can be accounted for by preparative considerations. The teflate ligand is routinely introduced using teflic acid ($HOSeF_5$) or $B(OTeF_5)_3$, but the analogous $B(OSeF_5)_3$ is unknown and $HOSeF_5$ is relatively unstable, difficult to prepare and undergoes redox reactions with most species except metal fluorides and oxides.¹ It has been shown that the teflate ligand can be introduced, oxidatively, into high-oxidation-state systems using $Xe(OTeF_5)_2$.^{10–13} We have been investigating the application of xenon difluoride for the introduction of the fluoride ligand into low-oxidation-state organometallic complexes,¹⁴ and here report our attempts to use $Xe(OTeF_5)_2$ and $Xe(OSeF_5)_2$ in analogous reactions including the synthesis of the first low-valent transition-metal seflate complexes.

Experimental

Carbon-13, ^{19}F and ^{125}Te NMR spectroscopies were carried out for dry dichloromethane solutions on a Bruker AM300 spectrometer at 75.47, 282.41 and 94.69 MHz respectively as described previously.³ Carbon NMR spectra were referenced to external $SiMe_4$, ^{19}F to external $CFCl_3$ and ^{125}Te to external neat $TeMe_2$ using the high-frequency positive convention. The IR spectra were recorded on a Digilab FTS40 Fourier-transform spectrometer at 4 cm^{-1} resolution for the complexes as Nujol mulls held between KBr discs, mass spectra on a Kratos Concept 1H mass spectrometer.

Selenium K-edge and rhenium L_{III}-edge EXAFS data were collected at the Daresbury Synchrotron Radiation Source at 2 GeV (*ca.* 3.2×10^{-10} J) with an average current of 190 mA in transmission mode, at room temperature, on stations 9:2 and 9:3 using a double-crystal Si(220) monochromator offset to 50% of the rocking curve for harmonic rejection. Samples were either diluted with dry boron nitride and mounted between Sellotape strips in 1 mm aluminium spacers or diluted with dry Teflon and mounted in pre-passivated FEP (perfluoroethylene-propylene copolymer) sample holders.¹⁵ The EXAFS data treatment utilised the programs EX¹⁶ and EXCURV 92.¹⁷ Five data sets were collected for each compound in *k* space, and averaged to improve the signal-to-noise ratio. The pre-edge background was removed by fitting the spectrum to a quadratic polynomial, and subtracting this from the whole spectrum. The

atomic contribution to the oscillatory part of the absorption spectrum was approximated using a polynomial, and the optimum function judged by minimising the intensity of chemically insignificant shells at low *r* in the Fourier transform. Curve fitting used single- or multiple-scattering curved-wave theory with phase shifts and back-scattering factors calculated using normal *ab initio* methods.¹⁸ Ground state potentials of the atoms were calculated using Von Barth theory and phase shifts using Hedin–Lundqvist potentials. The fits discussed below are for model data compared to raw (background-subtracted) EXAFS, and no Fourier filtering or smoothing has been applied. The distances and Debye–Waller factors were refined for all the shells, as well as the Fermi energy difference.

All preparative manipulations were carried out on a metal vacuum line with facilities to connect Teflon and FEP reaction vessels. The $[Mn_2(CO)_{10}]$ and $[Re_2(CO)_{10}]$ (Aldrich) were used as supplied, $Xe(OTeF_5)_2$ ¹⁹ and $Xe(OSeF_5)_2$ ²⁰ were prepared by the literature routes and dichloromethane was dried by refluxing over CaH_2 and stored over molecular sieves.

In a typical experiment, the metal carbonyl (*ca.* 0.1 mmol) was loaded, in a dry-box, into a pre-passivated FEP tube (6 mm outside diameter) fitted with a poly(tetrafluoroethylene) valve. The xenon reagent (*ca.* 0.1 mmol) was loaded similarly into a second FEP tube. After evacuation on a metal line, the xenon reagent was dissolved in dry dichloromethane (1 cm³) and then the solution decanted onto the metal carbonyl at -78°C . No immediate reaction occurred, but on warming to *ca.* 0°C a steady reaction ensued with the liberation of a spectroscopically silent condensable gas (confirmed as xenon by mass spectrometry). When the reaction was judged to have finished (Mn , *ca.* 2 min; Re , *ca.* 10 min) all volatile materials were removed *in vacuo*, the products recrystallised from dichloromethane and transferred to the dry-box and stored in a closed FEP tube for characterisation. Yields, typically 75–80%.

$[Mn(OTeF_5)(CO)_5]$: orange solid. Mass spectrum (EI): 436 (M^+) and 408 ($[M - CO]^+$). IR: 2156w, 2061s, 2025s, 848m, 777w, 674s, 627s and 542w cm^{-1} . NMR: ^{19}F , AB_4 spectrum, δ -30.8 [1 F, m, $^2J(FF) = 180$, F_{ax}] and -44.7 [4 F, m, $^2J(FF) = 180$, $^1J(TeF) = 3643$ Hz, F_{eq}].

$[Re(OTeF_5)(CO)_5]$: colourless solid. Mass spectrum (EI): 566 (M^+) and 536 ($[M - CO]^+$). IR: 2165w, 2041s, 2002s, 1207w, 940w, 914w, 679s, 593s, 555w cm^{-1} . NMR: ^{19}F , AB_4 spectrum, δ -32.6 [1 F, m, $^2J(FF) = 182$, F_{ax}] and -48.7 [4 F, m, $^2J(FF) = 182$, F_{eq}]; ^{125}Te , δ 569 [d of qnt, $^1J(TeF_{ax}) = 3135$, $^1J(TeF_{eq}) = 3648$ Hz].

$[Mn(OSeF_5)(CO)_5]$: orange solid. Mass spectrum (EI): 302 ($[M - 3CO]^+$), 274 ($[M - 4CO]^+$) and 195 ($[Mn(CO)_5]^+$). IR: 2164s, 2064s, 2029s, 864s, 683s, 593w and 543s cm^{-1} . NMR: ^{19}F , AB_4 spectrum, δ 101.7 [1 F, qnt, $^2J(FF) = 227$, F_{ax}] and 69.2 [4 F, d, $^2J(FF) = 227$, $^1J(SeF) = 1265$ Hz, F_{eq}].

$[Re(OSeF_5)(CO)_5]$: orange solid. Mass spectrum (EI):

Table 1 Infrared $\nu(\text{CO})$ data (cm^{-1}) for $\text{MX}(\text{CO})_5$ complexes

X	Mn				Ref.	Re				Ref.
	A ₁	E	A ₁	E		A ₁	E	A ₁	E	
OSeF ₅	2164	2064	2029	2025	This work	2168	2045	1986	2002	This work
OTeF ₅	2156	2061	2025	2025	This work	2165	2041	2002	2002	This work
ClO ₄	2158	2074	2023	2023	2					
O ₂ CCF ₃	2149	2063	2012	2012	25	2166	2059	2004	2004	26
Cl	2143	2005	2007	2007	2	2157	2046	1985	1985	2
Br	2138	2052	2007	2007	2	2150	2050	1990	1990	27
I	2129	2045	2008	2008	2	2150	2045	1990	1990	27

517.8340 (M^+), Calc. for $\text{C}_5\text{F}_5\text{O}_6^{187}\text{Re}^{80}\text{Se}$ 517.8340. IR: 2168w, 2045s, 1986w, 856s, 722m, 686s, 592s, 555s, 505w and 492s cm^{-1} . NMR: ^{19}F , AB₄ spectrum, δ 98.9 [1 F, qnt, $^2J(\text{FF}) = 232$, F_{ax}] and 64.1 [4 F, d, $^2J(\text{FF}) = 232$, $^1J(\text{SeF}) = 1277$ Hz, F_{eq}]; ^{13}C , δ 180.5 and 178.9.

Results and Discussion

In marked contrast to the oxidation of $[\text{M}_2(\text{CO})_{10}]$ ($M = \text{Mn}$ or Re) with XeF_2 which is difficult to control and gives either an uncharacterisable mixture of products (Mn)²¹ or the mixed-valence $[\text{Re}(\text{CO})_5(\mu\text{-F})(\text{ReF}_5)]$,²² oxidation with $\text{Xe}(\text{OTeF}_5)_2$ proceeds cleanly to give the same type of product, $[\text{M}(\text{OTeF}_5)(\text{CO})_5]$ ($M = \text{Mn}$ or Re). The spectroscopic data correlate exactly with those reported previously for these complexes, as prepared by methyl–teflate exchange reactions with teflic acid.²

The analogous methyl–seflate exchange reactions with HOSeF_5 do not appear to have been investigated. However, in view of the established redox sensitivity of sefflic acid, it is unlikely that this reaction would offer a viable route to organometallic seflate complexes. Indeed, the synthetic route to sefflic acid is far from straightforward.²³ Xenon bis[pentafluoro-oxoselenate(vi)], on the other hand, prepared from the reaction of SeOF_2 with XeF_2 ,²⁰ offers an alternative route into the coordination chemistry of the seflate ligand. The reactions of $[\text{M}_2(\text{CO})_{10}]$ ($M = \text{Mn}$ or Re) with $\text{Xe}(\text{OSeF}_5)_2$ proceed smoothly at around 0 °C in dichloromethane solution with the evolution of a spectroscopically silent, condensable, gas (xenon), to give the $[\text{M}(\text{OSeF}_5)(\text{CO})_5]$ ($M = \text{Mn}$ or Re) as moisture-sensitive orange solids. The products were characterised by NMR and IR spectroscopies and mass spectrometry.

The IR spectra for these complexes are similar and show three bands assignable to $\nu(\text{CO})$ as expected for a C_{4v} metal carbonyl unit. Table 1 allows a comparison of these IR data with those for complexes with related ' $\text{M}(\text{CO})_5$ ' ($M = \text{Mn}$ or Re) fragments which clearly shows that, in this system, the seflate ligand is a poorer donor ligand than chloride and teflate and similar to, or even weaker than, ClO_4^- or CF_3SO_3^- . The high $\nu(\text{Se-O})$ vibrations [864 (Mn) and 856 (Re) cm^{-1}] offer further evidence for the large degree of ionic character in the metal–oxygen bond. In metal and non-metal teflate compounds it is now well established that $\nu(\text{Te-O})$ varies with the degree of covalency in the element–oxygen bond.^{2,3} Although there are significantly fewer data on seflate derivatives, it would appear that $\nu(\text{Se-O})$ is also a sensitive probe for the ionic character of the metal–seflate interaction varying from 918 cm^{-1} ($[\text{NO}_2][\text{OSeF}_5]$)⁵ to 760 cm^{-1} ($\text{F}_5\text{SeOSeF}_5$).⁶ The ^{19}F NMR spectra reveal first-order AB₄ patterns with ^{77}Se satellites. It has been shown^{3–6} that the nature of the ^{19}F NMR spectra for metal–teflate and –seflate complexes gives a clear indication of the extent of the metal–ligand interaction and Table 2 clearly suggests that these low-valent metal seflate complexes have a very ionic M–O interaction as indicated by the vibrational data.

Unfortunately, we have been unable to grow crystals of these seflate complexes suitable for X-ray structural characterisation, but have shown that EXAFS can be a valuable technique for

Table 2 Fluorine-19 NMR data for compounds containing the seflate group

Compound	δ_A	δ_B	$^2J_{\text{AB}}/\text{Hz}$	Ref.
$[\text{NO}_2][\text{OSeF}_5]$	108.9	72.1	224	5
$[\text{Mn}(\text{OSeF}_5)(\text{CO})_5]$	101.7	69.2	227	This work
$[\text{Re}(\text{OSeF}_5)(\text{CO})_5]$	98.9	64.1	232	This work
$\text{Hg}(\text{OSeF}_5)_2$	89.7	75.5	230	4
$\text{Rb}[\text{Br}(\text{OSeF}_5)_4]$	81.8	71.2	224	5
$\text{Xe}(\text{OSeF}_5)_2$	80.5	69.4	234	20
HOSeF_5	75.9	66.1	227	23
$\text{F}_5\text{SeO}_2\text{SeF}_5$	55.2	54.1	230	6
$\text{F}_5\text{SeOSeF}_5$	62.7	76.0	226	6

obtaining structural data in the absence of single crystals²⁴ and so have recorded selenium K-edge and rhenium L_{III}-edge EXAFS data for these complexes; it has been impossible to acquire manganese K-edge EXAFS data because, as a result of the extreme moisture sensitivity of the manganese–seflate and –teflate derivatives, it has been necessary to seal them in our previously described pre-passivated FEP sample holders,¹⁵ which absorb virtually all the X-rays at the relatively soft manganese K-edge.

The reliability of the data collection and treatment at the selenium K-edge was established by analysis of the data for the only crystallographically characterised seflate compound, $\text{Xe}(\text{OSeF}_5)_2$.²⁸ The choice of this compound is far from ideal since its spectroscopic data suggest a highly covalent Xe–O bond and hence a relatively long Se–O bond distance, whereas our data for $[\text{M}(\text{OSeF}_5)(\text{CO})_5]$ ($M = \text{Mn}$ or Re) suggest highly polar M–O bonds. Furthermore, in the crystal there is orientational disorder of the oxygen and fluorine atoms (the molecule lying on a three-fold axis) and the X-ray data were, consequently, analysed on the basis of a molecular model with some constraints. This resulted in a Se–O bond length of 1.53 Å which is small in comparison with other Se–O bond lengths,^{29,30} and for which the authors state 'probably it is unrealistically small because of the constraints imposed with our model'. It proved to be impossible to distinguish by EXAFS between the oxygen and fluorine shells, which offers further support for the unreasonable crystallographically determined Se–O bond length since we have shown that EXAFS can distinguish between M–O and M–F shells separated by as little as 0.13 Å.³¹ Hence, the data ($k = 3\text{--}13 \text{ \AA}^{-1}$) were modelled to a two-shell fit (6F, 1Xe), the shells added stepwise, iterated in the usual way and the best fit tested for statistical significance.^{32,33} The Se–F distance compares well with the weighted average of the crystallographically determined Se–F and Se–O distances and is similar to these distances determined for $\text{Se}_2\text{OF}_{10}$ (Se–O 1.697, average Se–F 1.681 Å) in the gas-phase by electron diffraction.³¹ The non-bonded Se...Xe distance is also in good agreement with the distance calculated from the structural data [Table 3, Fig. 1(a)].

Transmission selenium K-edge EXAFS were then collected for $[\text{M}(\text{OSeF}_5)(\text{CO})_5]$ ($M = \text{Mn}$ or Re) out to $k = 15 \text{ \AA}^{-1}$ ($k = \text{photoelectron vector}$) beyond the edge but, due to poor signal-to-noise ratio at high k , the data were truncated at $k = 13 \text{ \AA}^{-1}$.

Table 3 Selenium K-edge EXAFS data^a

Compound	$d(\text{Se-F/Se-O})/\text{\AA}$	$2\sigma^2/\text{\AA}^2$	$d(\text{Se}\cdots\text{M})/\text{\AA}$	$2\sigma^2/\text{\AA}^2$	$d(\text{Se}\cdots\text{E})^c/\text{\AA}$	$2\sigma^2/\text{\AA}^2$	Fermi energy/eV	Fit index ^d	R factor ^e
Xe(OSeF ₅) ₂	1.695(1)	0.007(1)	3.299(6)	0.005(1)	3.334(6) ^f	0.003(2)	−9.2(4)	1.33	14.9
Xe(OSeF ₅) ₂ ^g	1.67 ^h	—	3.24 ⁱ	—	3.50 ^{fi}	—	—	—	—
[Re(OSeF ₅)(CO) ₅]	1.702(2)	0.006(1)	3.540(20)	0.004(2)	3.413(16)	0.001(3)	−17.6(4)	3.80	24.8
[Mn(OSeF ₅)(CO) ₅]	1.709(1)	0.007(1)	3.401(8)	0.008(2)	2.967(23)	0.003(5)	−8.7(3)	1.72	15.9

^a Standard deviations in parentheses; AFAC (a factor compensating for the reduction in amplitude due to multielectron processes) = 0.86 for all refinements. The systematic errors in bond distances arising from the data collection and analysis procedures are *ca.* ± 0.02 \AA for the first co-ordination shells and *ca.* ± 0.04 \AA for subsequent shells. ^b Debye–Waller factor. ^c Non-bonded distance to adjacent atoms, E = C unless otherwise indicated. ^d $\sum_i [(\chi^T - \chi^E)k_i^3]^2$. ^e $[(\chi^T - \chi^E)k^3 dk/dk]/[\chi^E k^3 dk/dk] \times 100\%$. ^f E = F. ^g X-Ray data taken from ref. 28. ^h Average bond distance (see text). ⁱ Calculated from data in ref. 28.

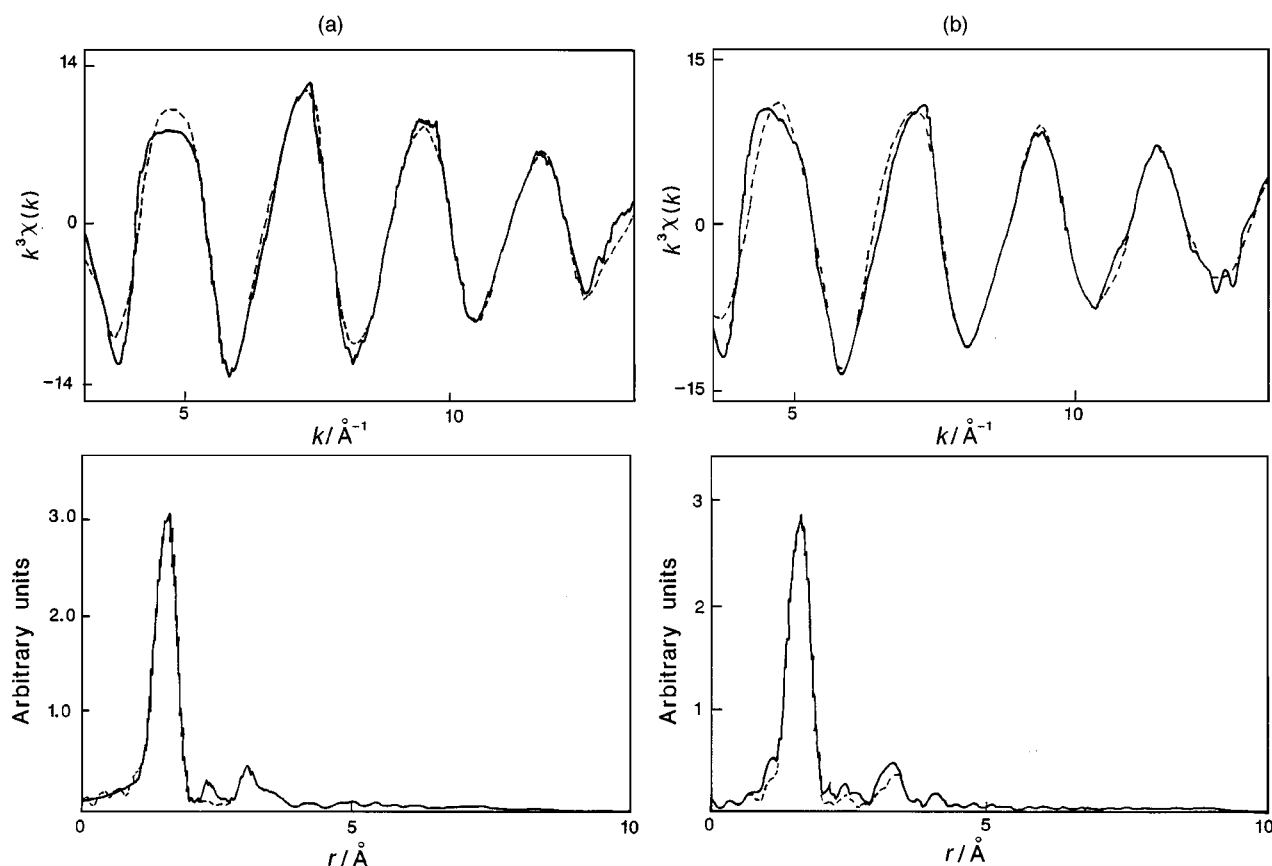


Fig. 1 Background-subtracted EXAFS (—, experimental $\times k^3$; ---, curved-wave theory $\times k^3$) and the Fourier transform (—, experimental; ---, theoretical) for (a) Xe(OSeF₅)₂ and (b) [Mn(OSeF₅)(CO)₅]; k is the photoelectron wave vector and r the radial distance from the absorbing atom

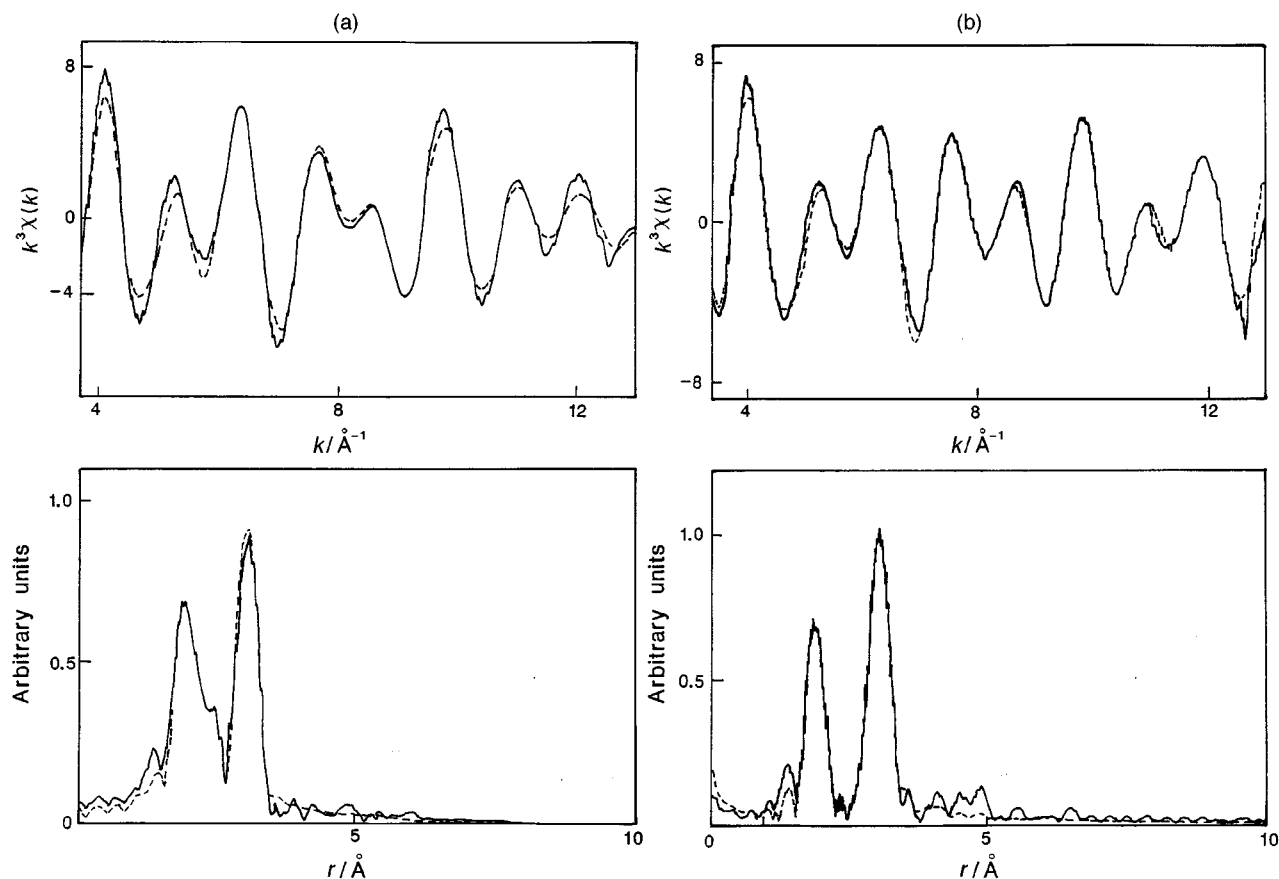
Several data sets on each compound were averaged, and the data multiplied by k^3 to compensate for the fall off in intensity at higher k . As with the model compound, the Fourier transforms were dominated by a single shell at *ca.* 1.70 \AA which was modelled to six fluorine atoms; although in these models it was possible to fit the EXAFS by a two-shell model (1O, 5F), the similar Se–O and Se–F distances resulted in data which were very strongly correlated and we believe that it is more appropriate to model the data by a single (averaged) shell in the same way as for Xe(OSeF₅)₂. Both Fourier transforms also revealed a further set of backscatterers at around 3.5 \AA . The data were subsequently modelled by two shells [6F, 1M (M = Mn or Re)]. However, although the addition of the second shell resulted in large reductions in the fit indices and R factors, inspection of the EXAFS and Fourier transforms suggested that there were additional contributions to the backscattering in the range 3–3.5 \AA . These additional contributions were eventually modelled to backscattering from one metal-bound carbonyl ligand. The justification for this approach arises from the structural characterisation² of [Mn(OTeF₅)(CO)₅] where, as a result of the bridging angle (139°) at the teflate oxygen atom, an eclipsed

conformation of the teflate and carbonyl ligands is adopted to minimise steric repulsions between fluorine and carbon atoms; the Te–O–Mn–CO plane bisects the F–Te–F angle resulting in equidistant Mn \cdots F interactions (3.75 and 3.67 \AA) and short C \cdots F distances (3.41 and 2.98 \AA). The EXAFS were, therefore, modelled to three shells (6F, 1M, 1C) [Table 3, Fig. 1(b)] as before. The resulting Se \cdots C distances are not unreasonable assuming that the seflate and carbonyl ligands in [M(OSeF₅)(CO)₅] (M = Mn or Re) adopt a similar staggered conformation.

The reliability of the data collection and treatment at the rhenium L_{III}-edge was established by analysis of data for the crystallographically characterised [ReCl(CO)₅] as a model compound.³⁴ Although it is possible to distinguish between the axial and equatorial carbonyl groups by X-ray crystallography, it proved impossible to do so by EXAFS, and so the data ($k = 3$ –13 \AA^{-1}) were modelled to a three-shell fit (5C, 1Cl, 5O), including multiple scattering for the oxygen shell with a fixed M–C–O angle (180°). The Re–Cl, Re–C and C–O distances are in excellent agreement with the crystallographic data [Table 4, Fig. 2(a)].

Table 4 Rhenium L_{III}-edge EXAFS data^a

Compound	$d(\text{Re}-\text{C})/\text{\AA}$	$2\sigma^2/\text{\AA}^2$	$d(\text{Re}\cdots\text{O})/\text{\AA}$	$2\sigma^2/\text{\AA}^2$	$d(\text{Re}-\text{X})/\text{\AA}$	$2\sigma^2/\text{\AA}^2$	$d(\text{Re}\cdots\text{E})/\text{\AA}$	$2\sigma^2/\text{\AA}^2$	Fermi energy/eV	Fit index	<i>R</i> factor
[ReCl(CO) ₅]	2.001(2)	0.006(1)	3.125(2)	0.007(1)	2.482(2) ^b	0.003(1)	—	—	-13.9(2)	2.0	18.2
[ReCl(CO) ₅] ^c	1.997 ^d	—	3.124 ^d	—	2.515 ^b	—	—	—	—	—	—
[Re(OTeF ₅)(CO) ₅]	2.002(3)	0.006(1)	3.124(3)	0.010(1)	2.187(14) ^e	0.009(4)	3.533(6)	0.008(1)	-11.8(4)	3.2	20.8
[Re(OTeF ₅)(CO) ₅]	2.009(3)	0.002(1)	3.126(2)	0.004(1)	2.167(8) ^e	0.001(1)	3.641(16)	0.018(3)	-11.9(2)	3.2	22.4

^a Details as in Table 3; AFAC (a factor compensating for the reduction in amplitude due to multi-electron processes) = 0.71 for all refinements.^b X = Cl. ^c X-Ray data taken from ref. 34. ^d Average bond distances (see text). ^e X = O.**Fig. 2** Background-subtracted EXAFS (—, experimental $\times k^3$; —, curved-wave theory $\times k^3$) and the Fourier transform (—, experimental; —, theoretical) for (a) [ReCl(CO)₅] and (b) [Re(OTeF₅)(CO)₅]. Other details as in Fig. 1

Transmission rhenium L_{III}-edge EXAFS data for [Re(OTeF₅)(CO)₅] and [Re(OTeF₅)(CO)₅] were initially analysed to similar three-shell models (5C, 1O, 5O) using multiple scattering (M–C–O fixed at 180°) for the longer oxygen distance. The data for the carbonyl shells are very similar to those for the model compound, [ReCl(CO)₅]. However, as seen in the selenium K-edge EXAFS analysis, the Fourier transforms for these complexes indicated additional shells at longer distances. The addition of one further shell for each complex (1Te or 1Se) resulted in significantly better fits between the models and the experimental data [Table 4, Fig. 2(b)]. For [Re(OTeF₅)(CO)₅] this further shell is in good agreement with the same non-bonded distance established from the selenium K-edge data, offering further credence to the reliability of the analysis. Although additional peaks in the Fourier transforms could be modelled to the non-bonded Re \cdots F interactions at *ca.* 3.9 Å outlined above, the inclusion of additional shells at these distances did not result in significant reductions in the fit indices.

The combined selenium and rhenium EXAFS data, together with reasonable values for the Mn–O and Te–O distances taken from the crystallographically characterised [Mn(OTeF₅)(CO)₅]² allow the M–O–E (M = Mn or Re, E = Se or Te) bond angles to be calculated by triangulation. These angles 130 ± 6

(Mn/Se), 139 (Mn/Te), 130 ± 6 (Re/Se) and $137 \pm 6^\circ$ (Re/Te) are highly consistent, within the accuracy of the calculations, and are in concordance with the highly polar M–O interactions in these complexes indicated by the spectroscopic data.

Unfortunately, this oxidative route is not applicable to an extensive range of low-valent metal complexes. Although we have characterised the products from the reactions of [Ru₃(CO)₁₂], [Os₃(CO)₁₂], [Ir₄(CO)₁₂] and [M(CO)₃(PPh₃)₂] (M = Ru or Os) with XeF₂,¹⁴ we have been unable to obtain reproducible, interpretable results for the products of the reactions of any of these complexes with either Xe(OTeF₅)₂ or Xe(OTeF₅)₂. These results, together with the results from the reactions of [M₂(CO)₁₀] (M = Mn or Re) with XeF₂, offer further evidence for the differences in co-ordinating abilities of the fluoride and teflate/seflate ligand in low-valent metal systems.

Acknowledgements

We would like to thank the EPSRC (M. C. C., L. J. W.) and the Royal Society (E. G. H.) for financial support, the Director of the Daresbury laboratory for the provision of facilities and Dr. J. F. W. Mosslemans (Daresbury Laboratory) for assistance in collecting and analysing the EXAFS data.

References

- 1 K. Seppelt, *Angew. Chem., Int. Ed. Engl.*, 1982, **21**, 877.
- 2 S. H. Strauss, K. D. Abney, K. M. Long and O. P. Anderson, *Inorg. Chem.*, 1984, **23**, 1994; K. D. Abney, K. M. Long, O. P. Anderson and S. H. Strauss, *Inorg. Chem.*, 1987, **26**, 2638.
- 3 S. A. Brewer, L. A. Buggey, J. H. Holloway and E. G. Hope, *J. Chem. Soc., Dalton Trans.*, 1995, 2941; M. C. Crossman, E. G. Hope and G. C. Saunders, *J. Chem. Soc., Dalton Trans.*, 1996, 509.
- 4 K. Seppelt, *Chem. Ber.*, 1972, **105**, 2431.
- 5 K. Seppelt, *Chem. Ber.*, 1973, **106**, 1920.
- 6 K. Seppelt, *Chem. Ber.*, 1973, **106**, 157.
- 7 K. Seppelt and D. Nothe, *Inorg. Chem.*, 1973, **12**, 2727.
- 8 K. Seppelt, *Angew. Chem., Int. Ed. Engl.*, 1972, **11**, 723.
- 9 K. Seppelt, *Chem. Ber.*, 1975, **108**, 1823.
- 10 D. Lentz, H. Pritzkow and K. Seppelt, *Inorg. Chem.*, 1978, **17**, 1926.
- 11 D. Lentz and K. Seppelt, *Z. Anorg. Allg. Chem.*, 1980, **460**, 5.
- 12 L. Turowsky and K. Seppelt, *Z. Anorg. Allg. Chem.*, 1990, **590**, 37.
- 13 H. P. A. Mercier, J. C. P. Sanders and G. J. Schrobilgen, *J. Am. Chem. Soc.*, 1994, **116**, 2921.
- 14 S. A. Brewer, K. S. Coleman, J. Fawcett, J. H. Holloway, E. G. Hope, D. R. Russell and P. G. Watson, *J. Chem. Soc., Dalton Trans.*, 1995, 1073; S. A. Brewer, A. K. Bridson, J. H. Holloway, E. G. Hope, L. A. Peck and P. G. Watson, *J. Chem. Soc., Dalton Trans.*, 1995, 2945; S. A. Brewer, J. H. Holloway and E. G. Hope, *J. Chem. Soc., Dalton Trans.*, 1994, 1067.
- 15 A. K. Bridson, J. H. Holloway, E. G. Hope, W. Levason, J. S. Ogden and A. K. Saad, *J. Chem. Soc., Dalton Trans.*, 1992, 139.
- 16 A. K. Bridson, EX, A Program for EXAFS Data Reduction, University of Leicester, 1992.
- 17 N. Binsted, J. W. Campbell and S. J. Gurman, EXCURV 92, SERC Daresbury Laboratory, 1992.
- 18 S. J. Gurman, N. Binsted and I. Ross, EXCURVE, *J. Phys. C*, 1984, **17**, 143; 1986, **19**, 1845.
- 19 F. Sladky, *Inorg. Synth.*, 1986, **24**, 36.
- 20 K. Seppelt, D. Lentz and G. Klöter, *Inorg. Synth.*, 1986, **24**, 27.
- 21 S. A. Brewer, J. H. Holloway and E. G. Hope, unpublished work.
- 22 D. M. Bruce, A. J. Hewitt, J. H. Holloway, R. D. Peacock and I. L. Wilson, *J. Chem. Soc., Dalton Trans.*, 1976, 2230.
- 23 K. Seppelt, *Inorg. Synth.*, 1980, **20**, 38.
- 24 M. J. Atherton, K. S. Coleman, J. Fawcett, J. H. Holloway, E. G. Hope, A. Karaçar, L. A. Peck and G. C. Saunders, *J. Chem. Soc., Dalton Trans.*, 1995, 4029.
- 25 F. A. Cotton, D. J. Darensbourg and B. W. S. Kolthammer, *Inorg. Chem.*, 1981, **20**, 1287.
- 26 J. Nitschke, S. P. Schmidt and W. C. Troglor, *Inorg. Chem.*, 1985, **24**, 1972.
- 27 R. Colton and J. E. Knapp, *Aust. J. Chem.*, 1972, **25**, 9.
- 28 L. K. Templeton, D. H. Templeton, K. Seppelt and N. Bartlett, *Inorg. Chem.*, 1976, **15**, 2718.
- 29 H. Oberhammer and K. Seppelt, *Inorg. Chem.*, 1979, **18**, 2226.
- 30 H. Oberhammer and K. Seppelt, *Inorg. Chem.*, 1978, **17**, 1435.
- 31 W. Levason, J. S. Ogden, A. K. Saad, N. A. Young, A. K. Bridson, P. J. Holliman, J. H. Holloway and E. G. Hope, *J. Fluorine Chem.*, 1991, **53**, 43; S. A. Brewer, A. K. Bridson, J. H. Holloway, E. G. Hope, W. Levason, J. S. Ogden and A. K. Saad, *J. Fluorine Chem.*, 1993, **60**, 13.
- 32 R. W. Joyner, K. J. Martin and P. Meehan, *J. Phys. C*, 1987, **20**, 4005.
- 33 N. Binsted, S. L. Cook, J. Evans, G. N. Greaves and R. J. Price, *J. Am. Chem. Soc.*, 1987, **109**, 3669.
- 34 D. M. Adams, P. W. Ruff and D. R. Russell, *J. Chem. Soc., Faraday Trans.*, 1991, 1831.

Received 9th February 1998; Paper 8/01109E